Modeling of Normally-off AlGaN/GaN MOSHEMT for Biosensor Applications: Role of molar fraction on the sensing performance

Rajkumar Mandal[1],Rajesh Dey, Debasis Mukherjee[1*]

[1]Dept. of Electronics & Communication Engineering, Brainware University, Barasat, Kolkata-700125.

Abstract-Biosensors can detect wide range of biomolecule species including viruses, nucleic acids, DNA, RNA and proteins. Recently, biosensors are being used in food analysis, drug development, crime detection, medical diagnosis, environmental field monitoring and also for the study of biomolecule interaction[1].Bio-FETs have a potential of being used as label-free sensors for rapid detection of bacteria, protein with sufficiently high sensitivity and small limit of lower detection [2].Lately, AlGaN/GaN HEMTs have been explored for biosensing applications because biomolecules can easily attach to its surface, when AlGaN barrier layer is grown on top of GaN[1]. Electrical detection using Field Effect Transistors (FETs) is generally based on two approaches: (i) charge interaction effect and (ii) dielectric constant modulation effect [3].This work presents an analytical model of a bio-molecule-induced threshold voltage shift (ΔV_{th}) in a normally off AlGaN/GaN MOSHEMT. In the analytical model, the occupancy of biomolecules is characterized by using the dielectric modulation (DM) technique for label-free electrical detection. Dielectric modulation and the Poisson equation were utilized to calculate the effective capacitance in the cavity region and the threshold voltage. Consequently, the changes in the threshold voltage and the drain current of the device are used as the sensing metric for the detection of bio-molecules in the cavity region. Interestingly, the molar fraction of barrier layer of HEMT structure greatly contributes to the dielectric constant. The Aluminum molar fraction in AlGaN layer, in this case, is varied to study the effect on the sensitivity. Thus, the sensing behavior of the MOSHEMT has been modeled according to the variation of molar fraction in the barrier AlGaN layer.

Keywords- Biosensors, Bio-molecules, MOSHEMT.

Introduction :

There is a strong interest in the effect of technology on health monitoring and health diagnosis devices in the field of technical development. In recent times, electronic biosensors used to detect the presence of biomolecules have been leading field of research. There are numerous advantages of field-effect transistor (FET)-based biosensors, such as high sensitivity , high scalability, label-free,[4-6] real time detection, miniaturization, low cost and compatibility with metal oxide semiconductor (CMOS) complementary technology. Bergveld's induction of ion-sensitive field-effect transistors (ISFETs) has led to impressive developments in the biosensor research arena. ISFETs are pH sensitive and provide high sensitivity for charged biomolecules with improved performance; failure to detect new biomolecules has led to the notion of a dielectric-moduled field effect transistor (DMFET).Researchers have highlighted and demonstrated structural improvements to promote miniaturization, as well as high-sensitivity devices such as DM-FET gate-under-lap, DM-tunnel field-effect transistor (DM-TFET), DM-metal oxide four-gate semiconductor field-effect transistor (DM-MOSFET), and DM-metal oxide double-gate semiconductor field-effect transistor (DG-MOSFET). For the label free electrical detection of biomolecules such as proteins, enzymes, cells, DNA, 3 amino propyltri ethoxy silane (APTES), biotin, strep-tavidins etc., nanogap embedded FET, Si-nanowire FETs, car-bon nanotubes and graphene-based FETs have been shown among the various FET biosensors. Impacts of interface parameters (channel thickness, cavity duration and cavity thickness) on sensing parameters (threshold voltage shift, drain current variation)[7] have been modeled and analysed for different biosensor devices, such as DM-MOSFET junction, DM-MOSFET gate drain underlap, DM-DG-TFET, DG-TFET, DM-TFET, DM-MOSFET, DM-MOSFET, DM-

DG-TFET, DG-TFET, four-gate di-gate, DM TFET, MOSFET electric modulated, junction less DM-DG-MOSFET and Underlap FET.Parihar and Kranti have demon-strated a cavity module-lated field effect transistor (FET) with improved sensitivity to detect biomolecules for a double gate junction less (JL) transistor design.[8-9] .In extreme conditions such as high temperatures, high pressure or corrosive environments, however, silicon based sensors are not suitable for operation. Therefore, due to their chemical stability, high sensitivity, better control of electronic properties and

Robustness for the detection of ions, gases and polar liquids, large band gap materials such as gallium nitride are the most pre-ferred material systems for biosensing. A two dimensional electron gas (2DEG) is formed in the AlGaN / GaN hetero structure used as a HEMT at the heterojunction between the AlGaN and the GaN, which is located near the surface and is therefore highly sensitive compared to the conventionally used GaN-based FET.I have been working on AlGaN / GaN HEMT biosensors to detect different material forms, such as solution ions, gas molecules, antigens, DNA, glucose, uric acid, etc., as well as pH. In the literature explaining the sensing parameters (Vth, Id) for GaN-based HEMT and MOSHEMT biosensors, no analytical analysis on

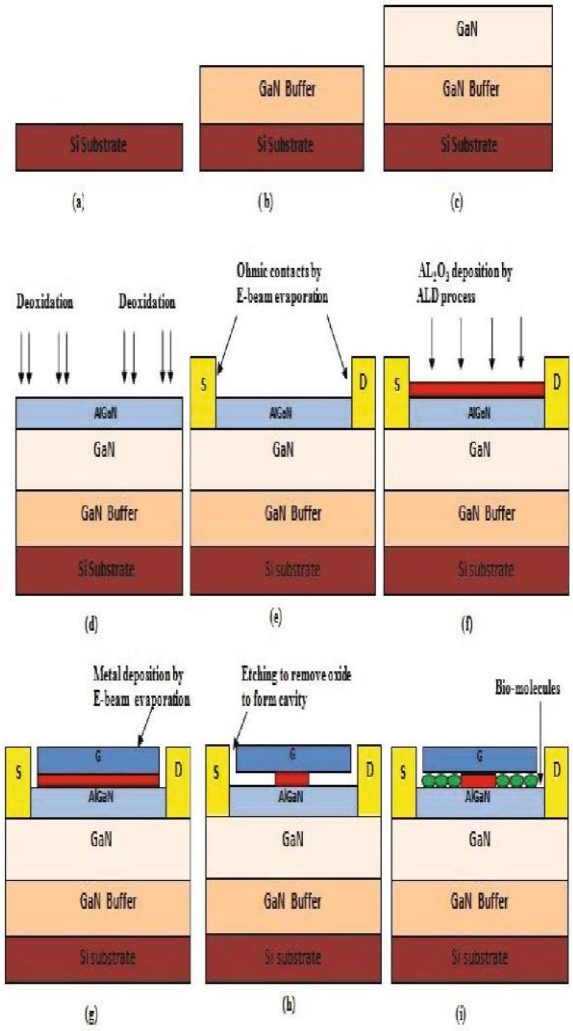

Fig. 1. (Color online) Process flow for the virtual fabrication of a dielectric-modulated normally-off AlGaN/GaN MOSHEMT by using a simulator.

The MOSHEMT has ever been recorded as obvious to the author's knowledge. A compact analytical model is built in this paper for a dielectric modulated (DM) normally off AlGaN / GaN MOSHEMT biosensor, and the results obtained using that model are compared with the results of the TCAD simulation. The process flow of output, along with the set-up of simulation, is defined in Sec. II. For Sec. III, the proposed device's mathematical model is developed. Inside Sec. IV,[10] the mathematical model equations developed are used in MATLAB for calculations and the results are compared with the results of the Synopsys TCAD simulation. The hypothesis is eventually presented in Sec. V.

Device Structure: In the graphic below, figure 1(a) illustrates the whole device structure of a MOSHEMT (the "AlGaN/GaN MOSHEMT") in which we have estimated that 25 nm of Al0.3Ga0.7N has been used on top of a 2 µm GaN buffer produced on a sapphire substrate.

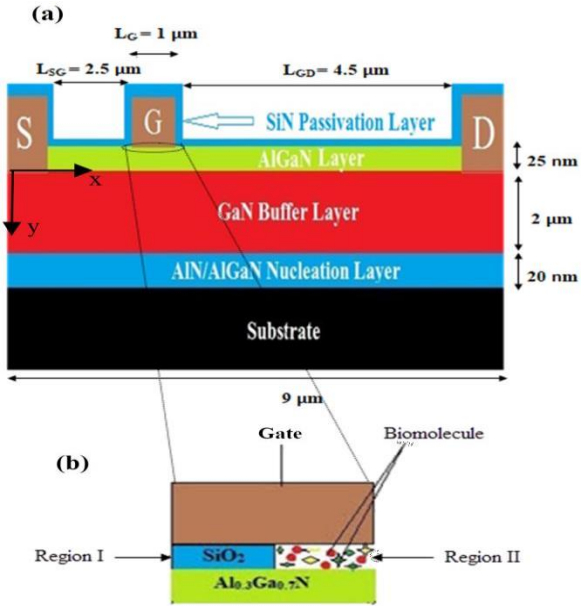

Fig. 2 (a) Structure of AlGaN/GaN MOSHEMT with nanogap cavity under the gate. (b) Expanded view of cavity region introduced below gate region.

Lattice mismatch between GaN buffer and substrate is said to be lessened by an AlN nucleation layer with a diameter of 20 nm. Schottky gate contact is formed from Ni/Au metal. Aluminum is used for the production of source and drain ohmic connections. In other words, the device is 8 µm long and 100 µm wide, except for the source and drain, which measure 0.8 µm and 100 µm correspondingly. Gate spacing is 4.0 µm for drain and gate space. In the following figure, the gate length (LG) is one nanometer and is placed near the source with a source to gate separation (LSG) of two and a half nanometers. To increase the drain current of the MOSHEMT device, the gate is considered near the source electrode.[11-13] Initially, the region below the gate was full of SiO2, and then, due to a 500 nm long (Lcavity) and 20 nm wide (Wcavity) nanogap cavity (shown in figure 2(b)) being considered in the region below the gate and on top of AlGaN, region II (shown in figure 2(b)) below the gate is now a location for biosequence detection. Authenticating that proper models and methods are adopted in TCAD simulation is crucial while calibrating. This study's choice of models and methodologies must be verified by comparing the simulation findings with those of Hu et al. The parameters of the simulation are maintained constant, as used by Hu et al. in their work on MOSHEMT (AlGaN/GaN) with AlGaN/GaN In Figure 2, the results are shown for a variety of gate voltages, and in Figure 3, the electric field is seen as a function of channel length. Experimental data reveals an excellent match between ID-VD[14] and output characteristics.

The simulation included a Shockley-Read-Hall (SRH) recombination model, a polarization model, calc.strain to determine the strain created, and albrct.n; these were the four main models employed. In order to determine the impact of velocity saturation in nitride groups, the FLDMOB model was applied.[15-16]

Result & Discussion: The ID-VG characteristics shown in figure 4 are obtained by introducing the biomolecules in the nanogap cavity region for Wcavity = 20 nm, Lcavity = 500 nm and by operation

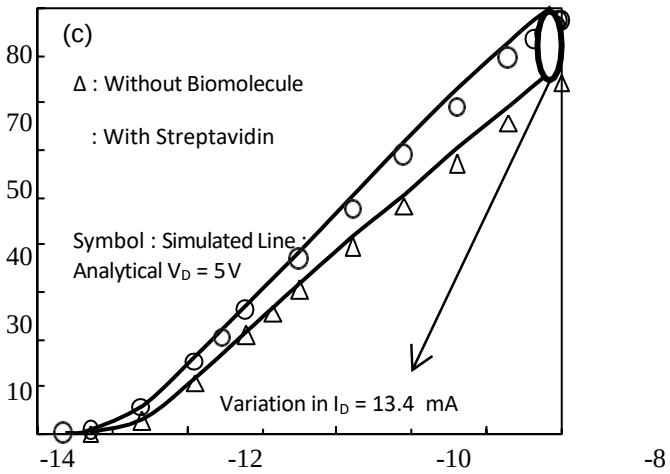

Table –I : Dielectric constant biomolecules

Biomolecule	Permittivity
Uricase	1.54
Streptavidn	2.1
Protein	2.50
ChOx	3.30

the device at a drain voltage of 5 V. Figure 4 shows variation of drain current with gate voltage for different biomolecules. The on state current increases with decrease in dielectric constant of biomolecules.[17] The on state current shows good sensitivity as it shows larger change in drain current above sub threshold regime. Figure 3 shows the change in drain current of the device for ChOx, uricase, streptavidin and protein. The dielectric constant of different biomolecules is shown in table I. The ChOx biomolecule shows a small variation of 4.3 mA in drain current but uricase with lesser dielectric constant shows larger change in drain current of 15.9 mA at a gate voltage of -7 V. To investigate the drain current of the proposed structure at various drain voltages, simulations have been carried out.

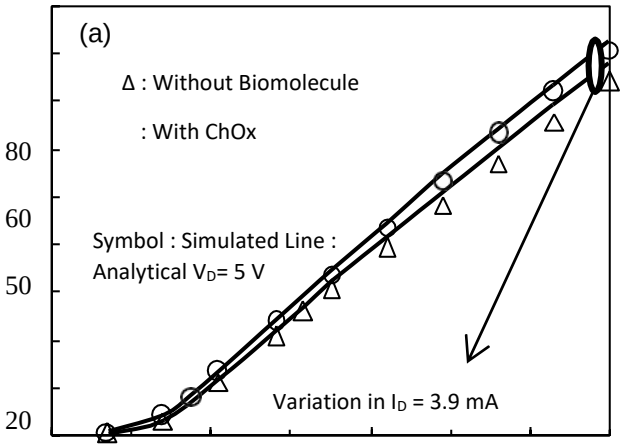

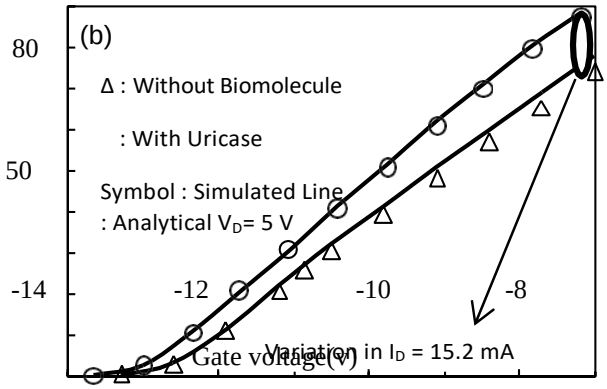

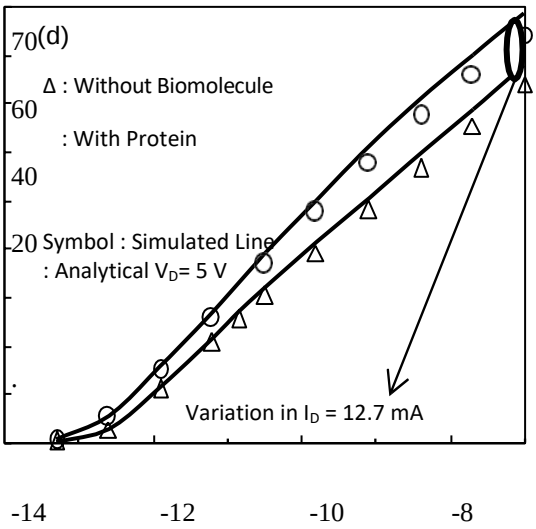

Fig. 3 ID (mA) –VG (V) for different biomolecules. (a) Variation of drain current for ChOx. (b) Variation of drain current for uricase. (c) Variation of drain current for streptavidin. (d) Variation of drain current for protein.

Simulated findings show agreement with analytical findings shown in Figure 4. An ID-VD feature reveals that uricase drains current the most, whereas ChOx shows the least variation. Various biomolecules demonstrate different SIon parameter changes.

Sion = [I (with biosensor)-I (without biosensor)]/ I (without biosensor)

When the cavity length is changed from 400 nm to 600 nm, a maximum change in sensitivity of 0.0158 is obtained for uricase. AlGaN provides for more surface to interact with biomolecules and enhances the charge density by modifying the drain current. Since uricase has a low dielectric constant, the

change is bigger for it. Thus, it follows that, for high sensitivity applications. Figure 4 shows how a change in cavity length from 400 nm to 600 nm cha nges the voltage threshold. [18]

As the cavity length is raised from 400 nm to 500 nm , roughly 0.2 V change in threshold voltage may be d etected using uricase.

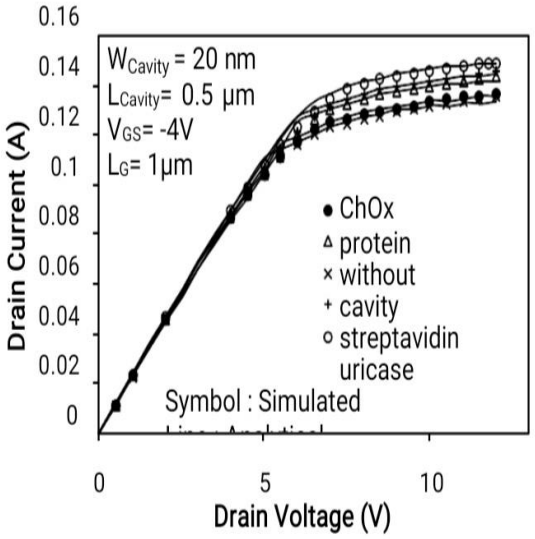

Fig. 4 ID(A)-VD(v) plot of simulated and analytical model for ChOx, protein, streptavidin and uricase biomolecules.[19]

as an optimization and identification parameter for bi omolecule species, the change in threshold voltage is also considered [20]

Conclusion

A model has been presented to identify biomolecule species based on analysis. The model predicts the AlGaN/GaN MOSHEMT device's behaviour for biosensing applications accurately. It is excellent in its attention to a wide range of biomolecules. A longer cavity causes drain-on sensitivity (SIon) to rise. The MOSHEMT is more sensitive than GAA-JLT in regard to drain current and threshold voltage. The capacitance of the gate source has changed, as well as the surface potential. One key element that our model overlooks is that our model is basic and does not account for elements that would be relevant in a real biosensing system. Conce ptually, however, we provide a fairly thorough quanti tative account of what is seen in the experiment. For t his reason, we expect our work to act as a catalyst for additional exploratory endeavors.

References:

[1] P. Pal, Y. Pratap, M. Gupta, and S. Kabra, IEEE Sensors Journal, Vol. 19, No. 2, 2018, pp. 587 – 593.

[2] N. Shafi, C. Sahu, and C. Periasamy, IEEE Sensors Journal, Vol. 20, No. 9, 2020, pp. 4749 – 4757.

[3] S. Kalra, M. J. Kumar, and A. Dhawan, IEEE Electron Device Letters, Vol. 37, No. 11, 2016, 1485 – 1488.

[4] A. L. Simonian, A. W. Flounders, and J. R. Wild, "FET- Based Biosensors for The Direct Detection of Organophosphate Neurotoxins," Electroanalysis, vol.16, no. 22, pp. 1896-1906, Nov.2004.

[5] N. Kazanskaya, A. Kukhtin, M. Manenkova, N. Reshetilov, L. Yarysheva, O. Arzhakova, A. Volynskii, and N. Bakeyev, "FET-based sensors with robust photosensitive polymer membranes for detection of ammonium ions and urea," Biosensors and Bioelectronics, vol. 11, no. 3 pp. 253-261, Jan.1996.

[6] A. R. Ruslinda, K. Tanabe, S. Ibori, X. Wang, and H. Kawarada, "Effects of diamond-FET-based RNA aptamer sensing for detection of real sample of HIV-1 Tat protein," Biosensors and Bioelectronics, vol. 40, no. 1, pp. 277-282, Feb.2013.

[7] D. Kim, Y. T. Jeong, H. J. Park, J. K. Shin, P. Choi, J. H. Lee, and G. Lim, "An FET-type charge sensor for highly sensitive detection of DNA sequence," Biosensors and Bioelectronics, vol. 20, no. 1, pp. 69- 74, Jul.2004.

[8] P. Bergveld, "The development and application of FET-based biosensors," Biosensors, vol. 2, no. 1, pp. 15-33, Jan.1986.

[9] J. Kim, J. H. Ahn, D. Moon, T. J. Park, S. Y. Lee, and Y. K. Choi, "Multiplex electrical detection of avian influenza and human immunodeficiency virus with an underlap-embedded silicon nanowire field-effect transistor," Biosensors and Bioelectronics, vol. 55, pp. 162-167, May.2014.

[10] C. Kim, C. Jung, K. B. Lee, H. G. Park and Y. K. Choi, "Label-free DNA detection with a nanogap embedded complementary metal oxide semiconductor," Nanotechnology, vol. 22, no. 13, pp. 135502, Feb.2011.

[11] K. Lee, S. J. Choi, J. H. Ahn, D. Moon, T. J. Park, S. Y. Lee, and Y. K. Choi, "An underlap field-effect transistor for electrical detection of influenza," Applied Physics Letters, vol. 96, no. 3, pp. 0337031- 0337033, Jan.2010.

[12] B. Gu, T. J. Park, J. H. Ahn, X. J. Huang, S. Y. Lee, and Y. K. Choi, "Nanogap field- effect transistor biosensors for electrical detection of avian influenza," small, vol. 5, no. 21, pp. 2407-2412, Nov.2009.

[13] I. Maesoon, J. H. Ahn, J. W. Han, T. J. Park, S. Y. Lee, and Y. K. Choi, "Development of a point-of-care testing platform with a nanogap-embedded separated double-gate field effect transistor array and its readout system for detection of avian influenza," IEEE Sensors journal, vol. 11, no. 2, pp. 351-360, Feb.2011.

[14] S. Deblina, H. Gossner, W. Hansch, and K. Banerjee, "Impactionization field-effect-transistor based biosensors

for ultra-sensitive detection of biomolecules," Applied Physics Letters, vol. 102, no. 20, pp. 2031101-2031105, May.2013.

[15] S. Deblina, and K. Banerjee, "Proposal for tunnel-field-effect-transistor as ultra-sensitive and label-free biosensors," Applied Physics Letters, vol. 100, no. 14, pp. 1431081-1431084, Apr.2012.

[16] M. Kenzo, T. Katsura, K. Kerman, Y. Takamura, K. Matsumoto, and E. Tamiya, "Label-free protein biosensor based on aptamer-modified carbon nanotube field-effect transistors," Analytical Chemistry, vol. 79, no. 2, pp. 782-787, Jan.2007.

[17] N. Kannan, and M. J. Kumar, "Charge-modulated underlap I-MOS transistor as a label-free biosensor: A simulation study," IEEE Transactions on Electron Devices, vol. 62, no. 8, pp. 2645-2651, Aug.2015.

[18] M. Salwa, I. Lee, S. K. Islam, S. A. Eliza, G. Shekhawat, V. P. Dravid, and F. S. Tulip, "Integrated MOSFET-embedded-cantilever-based biosensor characteristic for detection of anthrax stimulant," IEEE Electron Device Letters, vol. 32, no. 3, pp. 408-410, Mar.2011.

[19] A. M. Usman, O. Nur, M. Willander, and B. Danielsson, "Glucose detection with a commercial MOSFET using a ZnO nanowires extended gate," IEEE Transactions on Nanotechnology, vol. 8, no. 6, pp. 678-683, Nov.2009.

[20] H. Yuan, H. C. Kwon, S. H. Yeom, D. H. Kwon, and S. W. Kang, "MOSFET–BJT hybrid mode of the gated lateral bipolar junction transistor for C-reactive protein detection," Biosensors and Bioelectronics, vol. 28, no. 1, pp. 434-437, Oct.2011.